Int J Adv Manuf Technol (2017) 91:2267–2290
DOI 10.1007/s00170-016-9858-8

ORIGINAL ARTICLE

Modeling and optimization of turning process parameters during the cutting of polymer (POM C) based on RSM, ANN, and DF methods

A. Chabbi[1] · M.A. Yallese[1] · M. Nouioua[1] · I. Meddour[1] · T. Mabrouki[2] · François Girardin[3]

Received: 12 July 2016 / Accepted: 1 December 2016 / Published online: 3 January 2017

Abstract The present work concerns an experimental study dealing with cutting parameters' effects on the surface roughness, cutting force, cutting power, and productivity during turning of the polyoxymethylene (POM C) polymer. For that, a cutting tool made of cemented carbide was used. The work is divided into three steps. The first one deals with unifactorial tests, where the evolution of the machining parameters (roughness criteria, cutting force components, and cutting power) is investigated by varying cutting speed, feed rater, and depth of cut. The second part concerns the modeling of the output parameters: arithmetic roughness, cutting force, cutting speed, and material removal rate by using the results of a full factorial design (L_{27}). The second step concerns the adoption of the two modeling techniques, which are the response surface methodology (RSM) and the artificial neural network (ANN). The obtained results related to two both techniques are compared in order to discern the most efficient one. The last step of the present research work concerns the multi-objective optimization using the desirability function (DF). The optimization was carried out according to three approaches, which are the "quality optimization," "productivity optimization," and the combination between the quality and productivity.

Keywords Polymer POM C · Surface roughness · Cutting forces · MRR · Cutting power · ANOVA · RSM · ANN · Optimization

✉ A. Chabbi
amel_chabbi@yahoo.fr

M.A. Yallese
yallese.m@gmail.com

M. Nouioua
nouiouamourad25@yahoo.fr

I. Meddour
meddour26@yahoo.fr

T. Mabrouki
tarek.mabrouki@enit.utm.tn

François Girardin
francois.girardin@insa-lyon.fr

[1] Mechanical Department, Structure and Mechanics Laboratory (LMS), University May 8, 1945, P.O. Box 401, 24000 Guelma, Algeria

[2] ENIT, University of Tunis El Manar, Tunis, Tunisia

[3] Laboratoire Vibrations Acoustique, INSA-Lyon, 25 bis avenue Jean Capelle, 69621 Villeurbanne Cedex, France

1 Introduction

Polymers are increasingly used in industry because of several advantages such as low density, excellent corrosion resistance, mass production possibility, friction low coefficient, and the ability to be processed quietly and without external lubrication [1, 2]. Among the different types of polymers, thermoplastics are difficult to be cut due to their distinguished characteristics such as low elastic modulus, rate of moisture absorption, high coefficient of thermal expansion, and internal stresses [3]. As it can be noted in manufacturing processes, the integrity of finished surface is of great interest to qualify the quality of the workpiece. For that, surface roughness is an important parameter characterizing the technological quality of a product and a factor that greatly influences the manufacturing cost [4–6]. Also, it can be underlined that during the cutting of metal material, cutting power, dimensional accuracy, and chip formation are influenced by the evolutions of cutting force components [7–9].

In the case of the machining of different polymers, several researchers have studied also some process qualification criteria such as surface roughness, cutting forces, cutting power, and material removal rate. For instance, Xiao and Zhang [10] tried to assess the machinability of typical thermoplastic and thermosetting polymers and highlighted the effect of their viscous properties on the surface integrity, chip formation, and cutting forces. These authors noted that an increase in the cutting speed leads to improve the surface roughness. Nevertheless, at high cutting speed, the effect of temperature rise on the tool/workpiece interaction can be more significant than that of the strain rate.

Paulo Davim and Francisco Mata [11] evaluated the influence of glass fiber reinforcement during the turning of PA6 and PA66 GF30 polymers with cemented carbide tool (K15). The authors found that the presence of glass fiber PA66 GF30 polymer leads to higher values of cutting forces when compared to PA6 polymer.

Keresztes et al. [12] made a comparative study between cutting forces for different polymers such as PA6 (magnesium), PA6 (Na), polyoxymethylene (POM C), and the HD1000 (UHMWPE). They found that higher forces are obtained with the PA6 (Mg) and lowest ones with the HD1000 polymer. Cutting forces corresponding to the cutting of the POM C are almost the half of those recorded in PA6 (Mg), which is more hard resistant regarding cutting operation than the other three polymers.

M. Kaddeche et al. [13] studied surface roughness, cutting force, and temperature rise during the machining of two types of polymers: HDPE 80 and HDPE 100. They concluded that improved surfaces are obtained during the machining of HDPE 80 and surface roughness is affected by feed rate. Regarding cutting forces, increasing cutting speeds leads to lower cutting force components (*Fr*, *Fa*, and *Fv*) and *Fv* is the dominant component. They found that the temperature generated in the cutting zone is higher when cutting HDPE 80 than HDPE 100 and the depth of cut is the most influential factor on the temperature level.

Tushar U Jagtap et al. [14] proposed a review paper on the machining of polymers: cases of turning, milling, and drilling. The authors indicated that the behavior regarding machining of various polymers is not the same. For this purpose, the authors have suggested to study the effects of cutting parameters on different polymers, separately. The authors declared that the mechanical properties such as toughness, rigidity, abrasion resistance, and heat resistance of some polymers are similar those of metals. For that, these types of polymers can replace metals.

Manas Ranjan Panda et al. [15] investigated the influence of machining parameters on surface roughness and material removal rate in turning of nylon 6/6. Using the analysis of variance (ANOVA), they found that the surface roughness decreases with an increase of the cutting speed and decreases with the increase in the feed rate. The optimum process parameters yielding to optimal surface roughness are as follows: Vc = 1400 m/min, f = 0.1 mm/rev, and ap = 0.3 mm.

During the last years, statistical methods were adopted, among others, for the prediction of surface roughness and cutting forces during the machining of polymers. Indeed, Hasan Oktem et al. [16] have adopted artificial neural network (ANN) methodology for modeling and optimizing cutting parameters for minimum surface roughness during milling of POM C.

In the same way, V.N. Gaitond et al. [17] developed an ANN method to analyze the effect of work materials, tool materials, cutting speed, and feed rate on machining force, cutting power, and specific cutting force. They concluded that, when machining polyamide PA6 polymer, the specific cutting force is minimal at lower cutting speed and higher feed rate, whereas the specific cutting force is minimal at higher values of cutting speed and feed rate when cutting PA66 GF30.

D. Lazarevic et al. [18] proposed a study with the adoption of the Taguchi method to minimize the surface roughness during the turning of polyamide PA6. Using the analysis of variance (ANOVA) and ANOM, the authors showed that feed rate, f, is the most significant parameter followed by insert nose radius, r, and cutting depth, ap. It can be also mentioned that cutting speed, Vc, has no significant effect on the surface roughness evolution. These results regarding the effect of cutting parameters on surface roughness evolution were confirmed by M. Madic et al. [19] when adopting ANN methodology in the case of the machining of polyamide polymer.

When discussing the prediction capability of the improved harmony search algorithm (IHSA) and ANN methods for an optimization problem in the case of the turning of polyamide polymer, Madic et al. [20] declared that ANN can be efficiently used for mathematical modeling, whereas IHSA can be utilized to find the optimum cutting parameter settings.

In the field of machining of metallic materials and alloys, literature is abundant and widely available, but fewer research

Table 1 Physical and mechanical characteristics of POM C

Properties	Values
Density	1.41 g/cm^3
Absorption of moisture	0.2%
Resistance tensile	67 MPa
Module elasticity tensile	2800 MPa
Melting temperature	165 °C
Thermal conductivity	0.31 W/(m K)

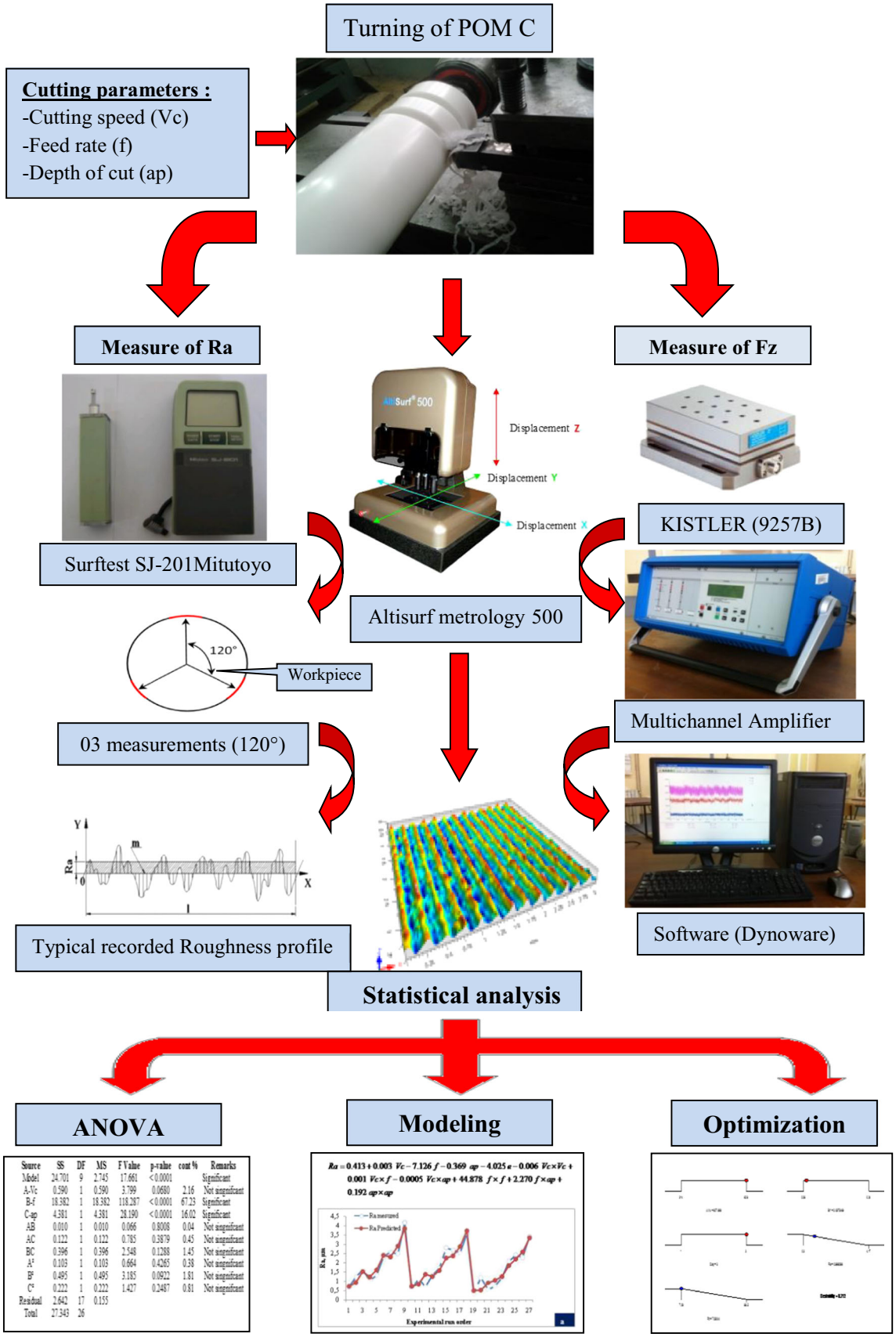

Fig. 1 Schematic diagram of the experimental setup

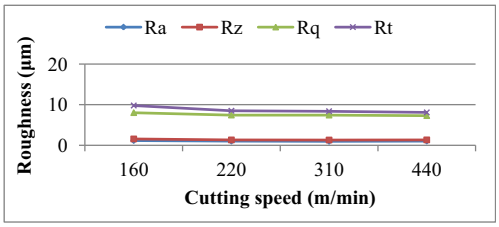

Fig. 2 Effect of cutting speed on the roughness (f = 0.12 mm/rev and ap = 1 mm)

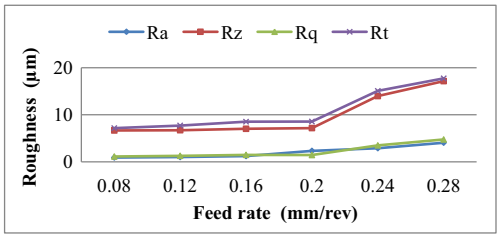

Fig. 4 Effect of f on the surface roughness (ap = 1 mm and Vc = 310 m/min)

works are carried out about polymer machining. Comparative literature in this field is very limited, particularly the machining of POM C.

In this contribution, firstly, we investigate the evolution of the technological parameters (roughness, cutting force, and cutting power) as a function of the cutting condition variations (Vc, f, and ap), during the turning of the polymer (POM C). Secondly, the modeling of the cutting process parameters using the response surface methodology (RSM) and ANN methods is carried out. Finally, optimizations of the cutting conditions using the desirability function (DF) according to three objectives (quality, productivity, and quality + productivity, simultaneously) are performed.

2 Experimental procedure

2.1 Workpiece material, cutting insert, and tool holder

The material used in this study is the POM C polymer. This material has important characteristics such as low moisture absorption, high hardness, high rigidity, good toughness, and impact resistance, even at high temperatures, and a high resistance to fatigue. It is widely employed for many applications such as gears, wheels, and bearings.

The physical and mechanical properties of POM C are given in Table 1. The workpieces are rods with a diameter of 80 mm with several grooves equally separated by 20 mm in length.

2.2 Measurement setup

Surface roughness was obtained instantly after each pass roughing by means of a Mitutoyo Surftest SJ-201 roughness meter. To prevent errors and recovery for more precision, roughness measurement was performed directly on the workpiece without dismounting it from the lathe. The measurements were repeated three times on three axial cylinder lines separated at 120°. The measurement of surface roughness is carried out according to the ISO 4287 standard. The tool holder is mounted on a three-component piezoelectric dynamometer (Kistler 9257B) allowing measurements from −5 to 5 KN. The measurement chain includes a charge amplifier (Kistler 5019B130) data acquisition hardware (A/D 2855A3) and graphical programming environment (DYNOWARE 2825A1-1) for data analysis and visualization. Those instruments are made by Kistler Company.

To properly characterize the surface roughness of the workpiece, several measurements based on 3D optical metrology platform modular 500 Altisurf were made. The cutting forces were measured in real time with a Kistler three-component dynamometer model 9257B linked via a multichannel charge amplifier (type 5011B) to high-impedance cable. The illustration of measured forces and surface roughness is given in Fig. 1.

2.3 Planning of experiments

To study the effect of various cutting parameters (Vc, f, ap) on the surface roughness and cutting force, a factorial design of four factors was adopted and each factor has four levels.

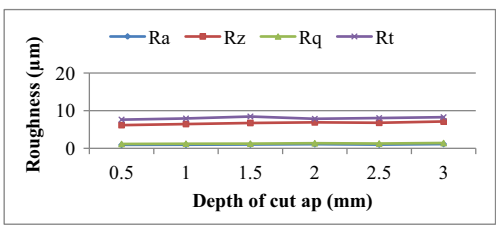

Fig. 3 Effect of ap on the roughness (Vc = 310 m/min and f = 0.12 mm/rev)

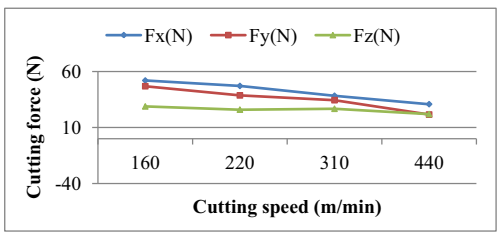

Fig. 5 Effect of Vc on the cutting force (ap = 1 mm and f = 0.12 mm/rev)

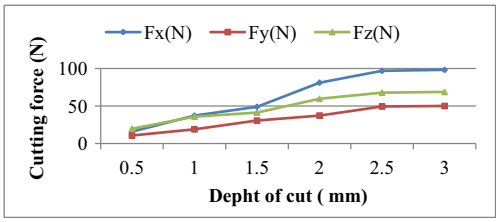

Fig. 6 Effect of *ap* on the cutting force (*Vc* = 310 m/min and *f* = 0.12 mm/rev)

The values chosen are as follows: cutting speed (220, 310, 440, and 500 m/min), feed rate (0.08, 0.12, 0.16, and 0.24 mm/rev), and depth of cut (0.5, 1, 1.5, and 2 mm). The levels of the cutting parameters are selected from the intervals recommended by the manufacturer of cutting tools.

2.4 Response surface methodology

The technique of RSM is an empirical modeling approach dictated to the determination of a relationship between various process parameters and responses. The objective is to explore the effect of these parameters on responses and optimize these responses [21] consequently.

In the current study, the relationship between cutting conditions and material machinability can be expressed as follows:

$$Y = \varphi(Vc, f, ap) \tag{1}$$

where φ is the response function and Y is the desired machinability aspect. In the present work, the RSM-based second-order mathematical model is given by the following:

$$Y = \alpha_0 + \sum_{i=1}^{k} \beta_i X_i + \sum_{i,j}^{k} \beta_{i,j} X_i X_j + \sum_{i=1}^{k} \beta_{ii} X_i^2 \tag{2}$$

where α_0 is the free term of the regression equation and the coefficients $\beta_1, \beta_2, \ldots, \beta_k$ and $\beta_{11}, \beta_{22}, \ldots, \beta_{kk}$ are the linear and the quadratic terms, respectively, while $\beta_{12}, \beta_{13}, \ldots, \beta_{k-1}$ are the interacting terms [23, 24, 30].

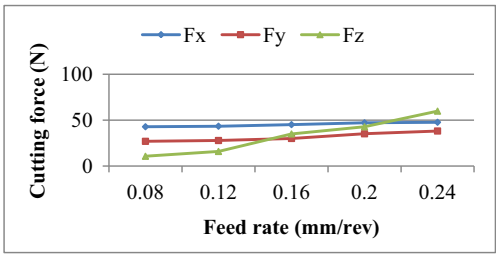

Fig. 7 Effect of *f* on the cutting force (*Vc* = 310 m /min and *ap* = 1 mm)

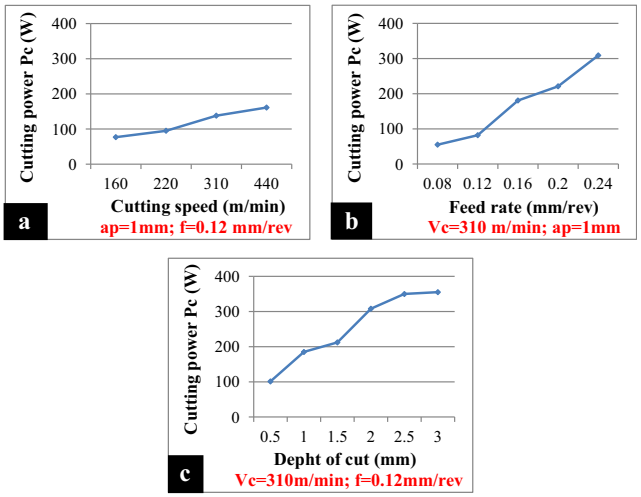

Fig. 8 Influence of cutting parameters on the cutting power

To determine the energy consumed during the machining operation, the cutting power *Pc* (W) related to the cutting force *Fz* (N) is measured. Another common output used to quantify the work provided is to calculate the material remove rate (MRR) (cm^3/min). The later can be defined as the volume of material removed divided by the machining time. Another way, MRR is to imagine an "instantaneous" material removal rate as the rate at which the cross-sectional area of the material being removed moves through the workpiece.

These aspects of machinability such as cutting power (*Pc*) and MRR are calculated with the obtained results by tangential force as follows:

$$Pc = \frac{Fz \times Vc}{60} \tag{3}$$

$$\text{MRR} = Vc \times f \times ap \tag{4}$$

where *Pc* is the cutting power (W), *Fz* is the tangential force (N), *f* is the feed rate (mm/rev), *ap* is the depth of cut (mm), *Vc* is the cutting speed (m/min), and MRR is the material removal rate (cm^3/min).

3 Results and discussion

3.1 Unifactorial tests

3.1.1 Effect of cutting parameters on surface roughness

Figures 2, 3, and 4 present the results of the evolution of different criteria for the surface roughness of POM C depending on the cutting conditions (*Vc*, *f*, and *ap*).

Figure 2 illustrates the evolution of the criteria (*Ra*, *Rq*, *Rz*, and *Rt*) as a function of the cutting speed (*Vc*). The machining

Table 2 Experimental results for *Ra*, *Fz*, *Pc*, and MRR

No.	Machining parameters			Response parameters			
	Vc (m/min)	*f* (mm/rev)	*ap* (mm)	*Ra* (μm)	*Fz* (N)	*Pc* (W)	MRR (cm^3/min)
1	314	0.08	1	0.67	22.38	117.12	25.12
2	314	0.08	2	1.22	29.12	152.39	50.24
3	314	0.08	3	1.61	34.99	183.11	75.36
4	314	0.16	1	1.40	28.50	149.15	50.24
5	314	0.16	2	1.61	41.63	217.86	100.48
6	314	0.16	3	1.98	50.45	264.02	150.72
7	314	0.24	1	2.02	32.67	170.97	75.36
8	314	0.24	2	2.58	53.41	279.51	150.72
9	314	0.24	3	3.14	66.60	348.54	226.08
10	440	0.08	1	0.56	19.70	144.47	35.20
11	440	0.08	2	1.13	22.98	168.52	70.40
12	440	0.08	3	1.07	30.82	226.01	105.60
13	440	0.16	1	1.13	24.28	178.05	70.40
14	440	0.16	2	1.22	39.48	289.52	140.80
15	440	0.16	3	1.79	47.11	345.47	211.20
16	440	0.24	1	1.98	28.08	205.92	105.60
17	440	0.24	2	2.18	39.94	292.89	211.20
18	440	0.24	3	3.01	56.41	413.67	316.80
19	628	0.08	1	0.47	10.99	115.03	50.24
20	628	0.08	2	0.87	18.46	193.21	100.48
21	628	0.08	3	1	27.09	283.54	150.72
22	628	0.16	1	1.03	20.94	219.17	100.48
23	628	0.16	2	1.16	32.35	338.60	200.96
24	628	0.16	3	1.42	42.18	441.48	301.44
25	628	0.24	1	1.65	21.33	223.25	150.72
26	628	0.24	2	2.01	32.97	345.09	301.44
27	628	0.24	3	2.98	47.48	496.96	452.16

is stable; there is a slight decrease in the various roughness criteria when the *Vc* increases from 160 to 310 m/min. This proves that in this interval, the cutting speed does not have a significant influence on the roughness. In practice, the increase in *Vc* of 160 to 310 m/min decreases the various roughness criteria (*Ra*, *Rq*, *Rz*, and *Rt*) of 13.24, 9.10, 16.67, and

Table 3 ANOVA result for surface roughness *Ra*

Source	SS	DF	MS	*F* value	*P* value	Cont % (%)	Remarks
Model	13.473	9	1.497	53.547	<0.0001		Significant
A-*Vc*	0.7363	1	0.736	26.330	<0.0001	5.28	Significant
B-*f*	9.2633	1	9.263	331.345	<0.0001	66.41	Significant
C-*ap*	2.748	1	2.748	98.283	<0.0001	19.70	Significant
AB	0.0001	1	0.0001	0.005	0.944	0.00	Not significant
AC	0.0105	1	0.010	0.377	0.547	0.08	Not significant
BC	0.187	1	0.187	6.707	0.019	1.34	Significant
A^2	0.0358	1	0.036	1.279	0.274	0.26	Not significant
B^2	0.404	1	0.404	14.446	0.001	2.90	Significant
C^2	0.017	1	0.017	0.598	0.450	0.12	Not significant
Residual	0.475	17	0.028				
Total	13.948	26					

Table 4 ANOVA result for tangential force *Fz*

Source	SS	DF	MS	*F* value	*P* value	Cont %	Remarks
Model	4481.948	9	497.994	99.975	<0.0001		Significant
A-*Vc*	623.751	1	623.751	125.221	<0.0001	13.66	Significant
B-*f*	1419.871	1	1419.871	285.047	<0.0001	31.09	Significant
C-*ap*	2073.715	1	2073.715	416.309	<0.0001	45.41	Significant
AB	33.967	1	33.967	6.819	0.018	0.74	Significant
AC	1.674	1	1.674	0.336	0.570	0.04	Not significant
BC	196.668	1	196.668	39.482	<0.0001	4.31	Significant
A^2	5.198	1	5.198	1.043	0.321	0.11	Not significant
B^2	63.202	1	63.202	12.688	0.002	1.38	Significant
C^2	1.395	1	1.395	0.280	0.603	0.03	Not significant
Residual	84.680	17	4.981				
Total	4566.628	26					

17.32%, respectively. Similar results were found by Gaitonde et al. [17] when machining a polymer.

Figure 3 shows the effect of the depth of cut (*ap*) on the surface roughness. It is easy to see that *ap* does not play a decisive role in the machined surface quality of POM C. With its increase, a slight increase in the values of the roughness criteria is observed. From a practical point of view, with the increase in *ap* of 0.5 to 3 mm, the different roughness criteria (*Ra*, *Rz*, *Rq*, and *Rt*) increase by 13.48, 19.30, 9.82, and 17.86%, respectively. This observation allows us to say that if we want maximum productivity and keep the same roughness, it is advantageous to increase *ap* since its influence is low on the surface roughness.

Figure 4 describes the evolution of the surface roughness criteria as a function of feed rate (f). It is noted that the state of the surface deteriorates with an increase of feed rate and this degradation is significant beyond $f = 0.2$ (mm/rev). An increase in feed rate from 0.08 to 0.28 (mm/rev) induces an increase in roughness criteria (*Ra*, *Rz*, *Rq*, and *Rt*) of 341.30, 157.51, 320.35, and 147.91%. It can be said that the effect of feed rate is the most important on the condition of the machined surface of the polymer POM C.

3.1.2 Effect of cutting conditions on cutting force

Figure 5 shows the evolution of the three components of the cutting force (*Fx*, *Fy*, and *Fz*) as a function of the cutting speed. It is clear that the three components decrease with the increase of *Vc*. When *Vc* increases from 160 to 440 m/min, the three components decrease by 68.74, 117.26, and 31.14%, respectively. This is due to the increase of the temperature in the cutting zone when the cutting speed increases, making the material more malleable and easy to machine [26].

Table 5 ANOVA result for the power *Pc*

Source	SS	DF	MS	*F* value	*P* value	Cont %	Remarks
Model	258,468.167	9	28,718.685	100.389	<0.0001		Significant
A-*Vc*	33,251.362	1	33,251.362	116.233	<0.0001	12.63	Significant
B-*f*	80,320.241	1	80,320.241	280.767	<0.0001	30.50	Significant
C-*ap*	125,900.59	1	125,900.59	440.098	<0.0001	47.81	Significant
AB	1431.590	1	1431.590	5.004	0.039	0.54	Not significant
AC	8075.110	1	8075.110	28.227	<0.0001	3.07	Significant
BC	9802.444	1	9802.444	34.265	<0.0001	3.72	Significant
A^2	372.768	1	372.768	1.303	0.269	0.14	Not significant
B^2	5132.276	1	5132.277	17.940	0.0005	1.95	Significant
C^2	15.837	1	15.837	0.055	0.817	0.01	Not significant
Residual	4863.259	17	286.074				
Total	263,331.426	26					

Table 6 ANOVA result for MRR

Source	SS	DF	MS	*F* value	*P* value	Cont % (%)	Remarks
Model	273,238.869	9	30,359.874	403.712	<0.0001		Significant
A-*Vc*	45,433.037	1	45,433.037	604.149	<0.0001	16.55	Significant
B-*f*	101,572.791	1	101,572.791	1350.670	<0.0001	37.00	Significant
C-*ap*	101,572.791	1	101,572.791	1350.67	<0.0001	37.00	Significant
AB	7670.579	1	7670.579	102	<0.0001	2.79	Significant
AC	7670.579	1	7670.579	102	<0.0001	2.79	Significant
BC	16,298.018	1	16,298.018	216.724	<0.0001	5.94	Significant
Residual	1278.430	17	75.202				
Total	274,517.299	26					

Figure 6 illustrates the evolution of the components of cutting force as a function of depth of cut (*ap*) during the turning of POM C. It will be noted that when *ap* increases by 0.5 to 3 mm, this leads to a successive increase in the three components of the cutting force (*Fx*, *Fy*, and *Fz*) of 520.49, 368.60, and 250.76% successively. With the increase of *ap*, the cross section of the removed chip becomes very large, which causes an increase in the volume of deformed material and requires significant cutting forces [26].

Figure 7 shows the evolution of the various criteria of the cutting forces as a function of feed rate (*f*). According to this figure, it can be observed that with the increase of feed rate (*f*) from 0.08 to 0.24 mm/rev, the cutting forces (*Fx*, *Fy*, and *Fz*) increase by 11.43, 41.66, and 460.97%, respectively, and this is due to the increase in cross section of the chip. It is also noted that beyond $f = 0.15$ mm/rev, the tangential force predominates the other two.

3.1.3 Effect of cutting conditions on the cutting power

Figure 8a–c shows the effect of cutting parameters on cutting power (*Pc*). Analysis of the results shows that the increase in *Vc*, *f*, and *ap* leads to an increase in *Pc*. This is logical since *Pc* is closely related to the cutting speed and cutting forces (Eq. 3). With the increase of *Vc* from 160 to 440 m/min, *Pc* increases by 109.69% (Fig. 8a). By increasing the feed rate (*f*) values from 0.08 to 0.24 mm/rev (Fig. 8b) and the depth of cut (*ap*) from 0.5 to 3 mm (Fig. 8c), the section of the chip increases, which implies greater breaking strength and cutting forces; this leads to an increase in cutting power. In this specific case, the cutting depth (*ap*) increase influences more the increase of the cutting power (*Pc*) about 2751%.

3.2 Statistical analysis

Table 2 shows all the values of the responses of factors: surface roughness (*Ra*) and cutting force (*Fz*), cutting power (*Pc*), and MRR. The objective is to analyze the influence of various combinations of levels of mixing function in cutting parameters (*ap*, *Vc*, *f*) with full factorial design on the total variance of the obtained results (*Ra*, *Fz*, MRR). The result of *Pc* was calculated based on Eq. 3. The surface roughness was obtained in the range of 0.47–3.14 μm; cutting force, cutting power, and MRR were obtained in the range of 10.99–66.6 N, 115.03–441.48 W, and 25.12–452.16 cm^3/min, respectively.

The analysis of variance (ANOVA) is a standard statistical technique that is commonly used in order to determine the significance of the independent variables on the output responses [22]. It does not analyze the data directly but determines the percentage of contribution of each factor in determining the variability (variance) of data.

Tables 3, 4, 5, and 6 illustrate the ANOVA results for surface roughness (*Ra*), cutting force (*Fz*), cutting power (*Pc*), and MRR, respectively, for a 95% confidence level. In these tables, the values of DoF, the sum of squared deviations (SS), mean square (MS), and percentage of contribution (cont %) of each model terms are listed. The main purpose is to analyze the influence of the cutting parameters (*ap*, *Vc*, *f*) on the total variance of the results. The values of "*P*" in the models are less than 0.05, indicating that the models are adequate and that the terms have a significant effect on the responses, which are desirable.

Table 3 shows the ANOVA results for roughness (*Ra*). We can see that *f* is the most important factor affecting *Ra*. Its contribution is 66.41%. The second important term affecting *Ra* is *ap* with 19.70% of contribution and *Vc* with 5.28%. The interaction ($f \times ap$) and product (f^2) have contributions of less than 1.5%. It can be assumed that the other terms are not significant. Similar results on the effect of feed rate on roughness have been reported by Q. Jiang et al. [24], M. Vijaya Kini, and A.M. Chincholkar [25] when turning of different polymers.

From the analysis of Table 4, it can be apparently seen that *ap* and *f* have a significant effect on *Fz*. It is clear that *ap* is the most significant factor associated for *Vc* with 45.41%. The next largest factor influencing *Fz* is *f* followed by *Vc*. Their contributions are 31.09 and 13.66% of the model. The

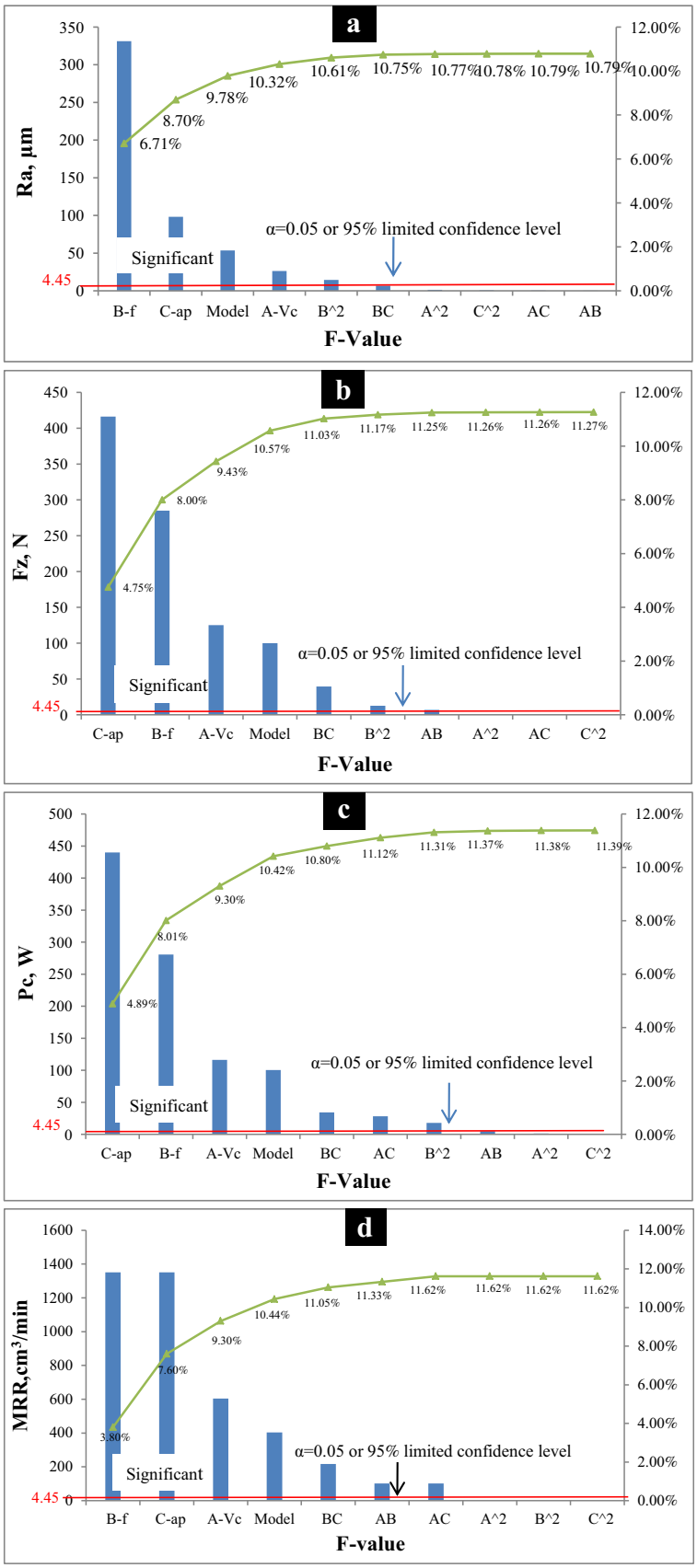

Fig. 9 Graphs of Pareto, for effect cutting parameters on **a** surface roughness, **b** cutting force, **c** power, and **d** material removal rate

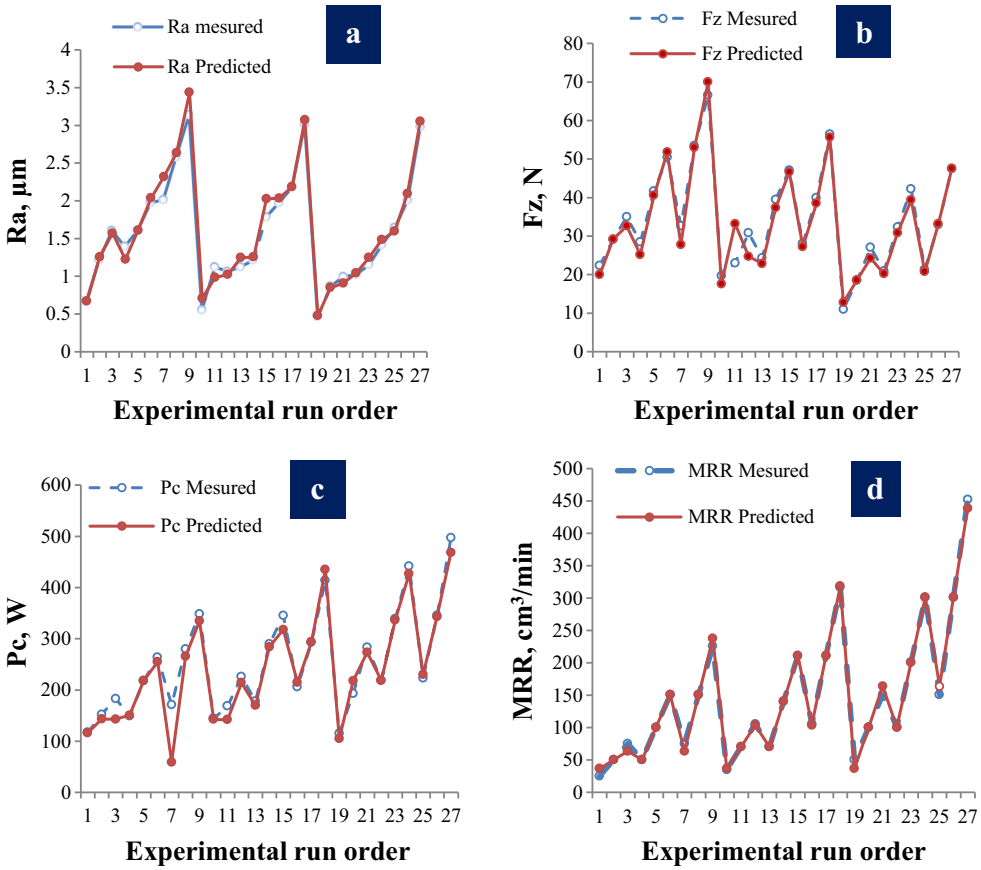

Fig. 10 Measured vs. predicted values of technological parameters: **a** surface roughness, **b** tangential force, **c** cutting power, and **d** material remove rate

interaction ($f \times ap$) has 4.31% of contribution and the term (f^2) has 1.38%. The other terms have a contribution lower than 1%. Similar result was found by Mohd Suhail Ansari et al. [26] and D. Lazarevićet al. [18] when turning polytetrafluoroethylene and polyamide polymer, respectively.

Table 5 indicates that all the input parameters are significant, but *ap* is the most significant factor followed by *f* and *Vc*. Their contributions are 47.81, 30.50, and 12.63%, respectively. The interactions ($Vc \times ap$, $f \times ap$) and the term (f^2) have contributions lower than 1%. Other terms do not have a significant meaning on *Pc*.

Table 6 presents the ANOVA results for the material removal rate (MRR). It can be stated that both *ap* and (*f*) have the highest statistical significance (37%) followed by *Vc* (16.55%). The interactions ($Vc \times f$, $Vc \times ap$, and $f \times ap$) are less important and vary between 5.94 and 2.79%.

In order to have better presentation of the obtained results, a Pareto graph is built (Fig. 9). This figure ranks the cutting parameters and their interactions of their growing influence on *Ra*, *Fz*, *Pc*, and MRR. The effects are standardized (*F* value) for a better comparison. Standardized values in this figure are obtained by dividing the effect of each factor by the error on the estimated value of the corresponding factor. The more the standardized effect, the higher the factor considered influence. If the *F* table values are greater than 4.45, the effects are significant. On the other hand, if the values of *F*-table are less than 4.45, the effects are not significant. The confidence interval chosen is 95%.

3.3 Modeling by response surface methodology

The relationship between the factors and the output parameters was modeled by quadratic regression. The regression equations obtained are given below by Eqs. (5), (6), (7), and (8) with coefficients of determination R^2 of 96.59, 98.15, 98.15, and 99.53%, respectively. These regression models are useful in predicting the response parameters with respect to the input control parameters.

$$\begin{aligned} Ra = {} & 2.016\text{–}4.047E\text{–}3 \times Vc\text{–}7.230 \times f + 0.019 \times ap \\ & +2.723E\text{–}4 \times Vc \times f\text{–}1.874E\text{–}4 \times Vc \times ap \\ & +1.563 \times f \times ap + 3.280E\text{–}6 \times Vc^2 + 40.538 \\ & \times f^2 + 0.053 \times ap^2 \end{aligned} \quad (5)$$

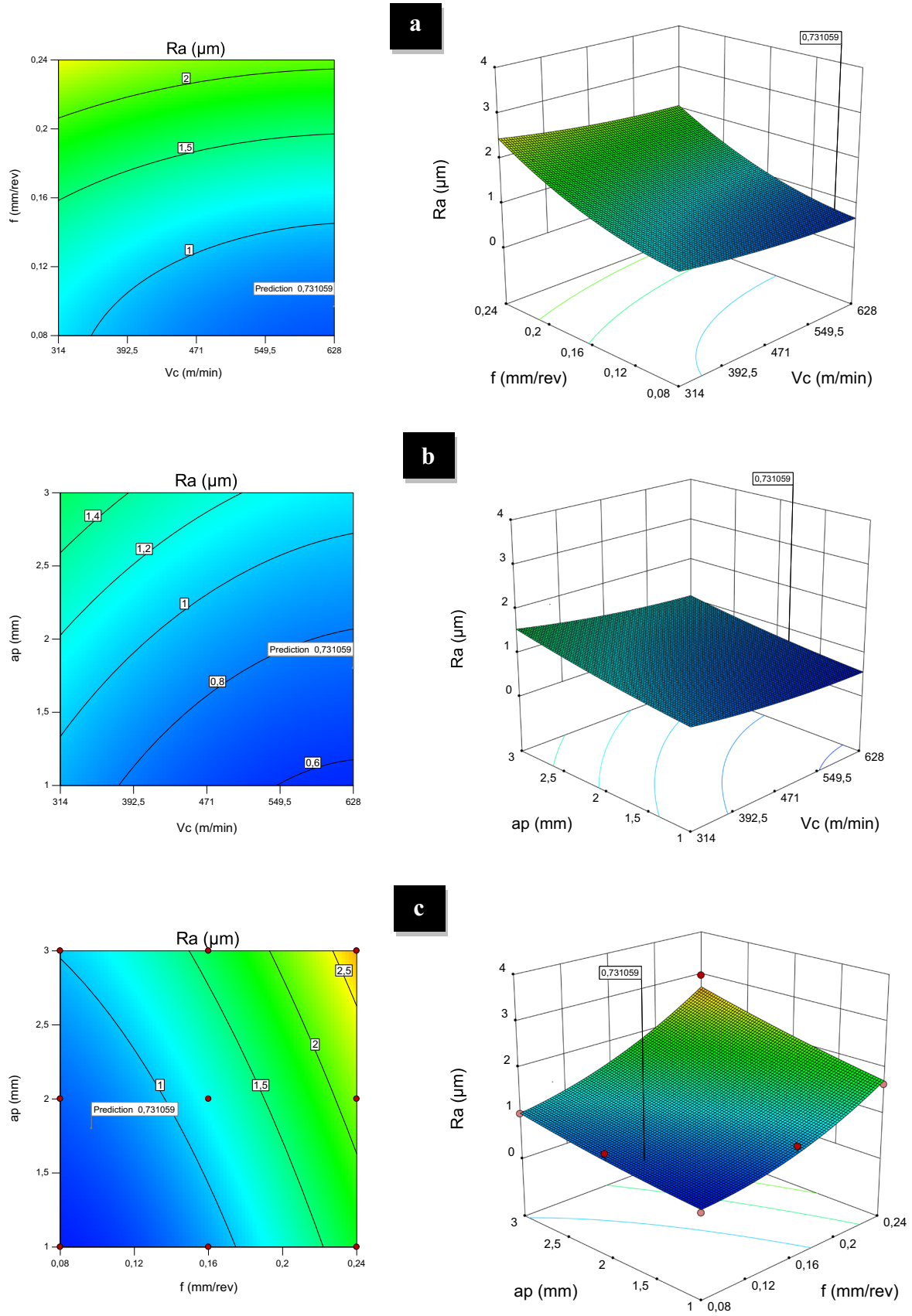

Fig. 11 Estimated response surface for surface roughness *Ra* depending on *Vc*, *f*, and *ap*

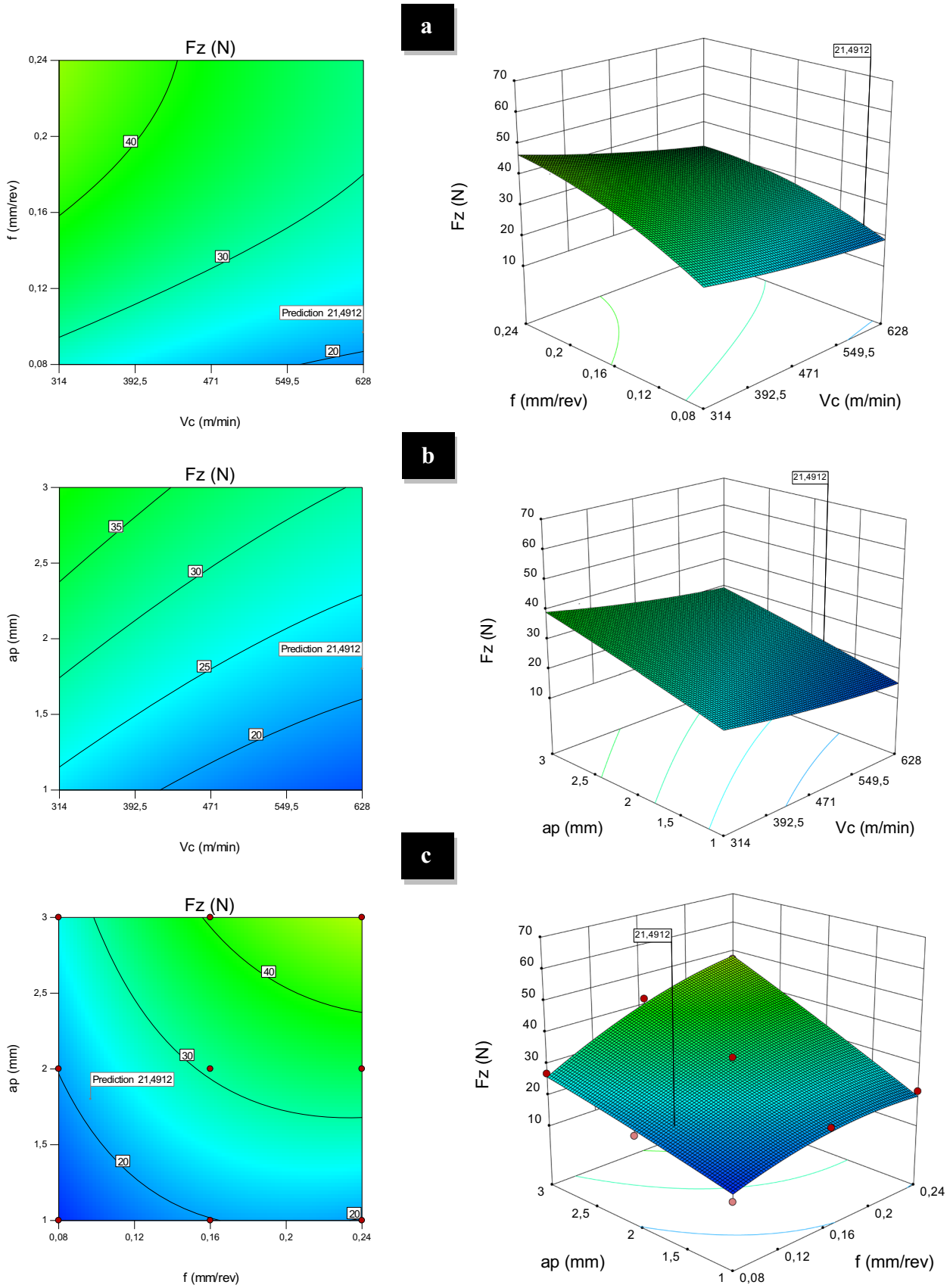

Fig. 12 Estimated response surface for tangential cutting force *Fz* depending on *Vc*, *f*, and *ap*

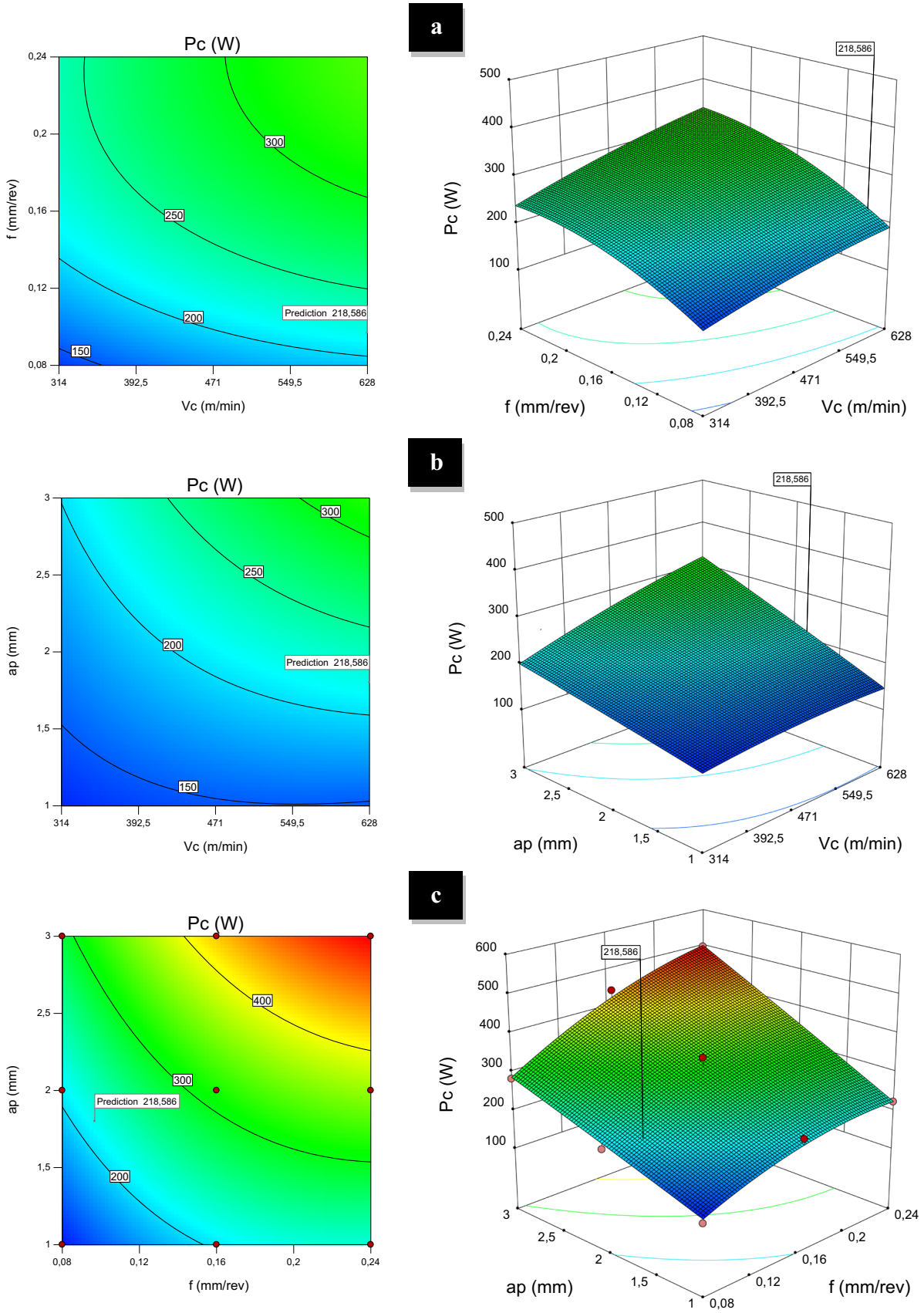

Fig. 13 Estimated response surface for power *Pc* depending on *Vc*, *f*, and *ap*

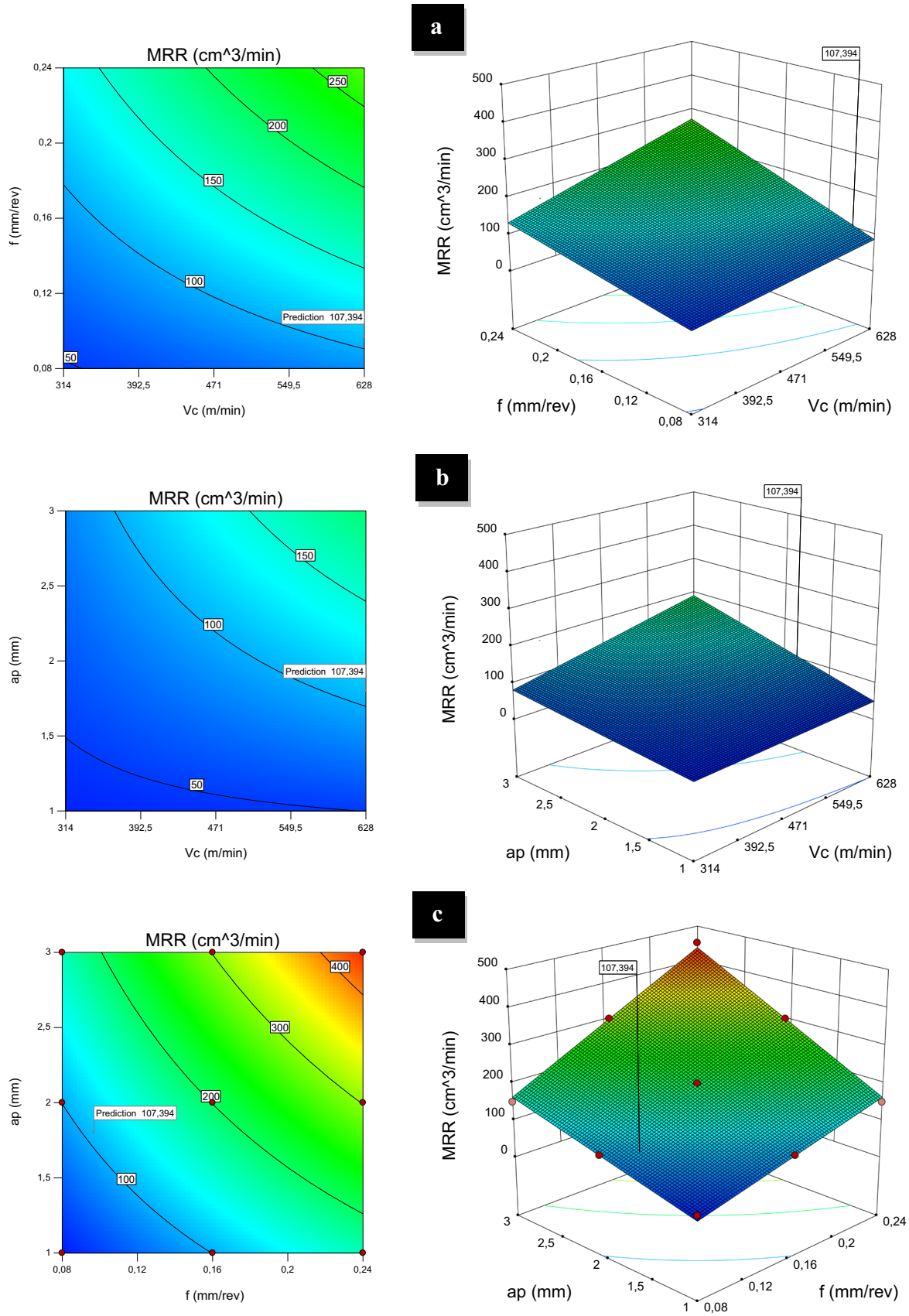

Fig. 14 Estimated response surface for MRR depending on *Vc*, *f*, and *ap*

Table 7 Confirmation experiments

Test	*Vc* (m/min)	*f* (mm/rev)	*ap* (mm)	Experimental value	Predicted value	Error % (%)
Surface roughness *Ra* (μm)						
1	360	0.14	1	0.99	1.003	1.38
2	534	0.08	2	0.76	0.782	2.94
3	534	0.14	2	1.22	1.266	3.78
Cutting force *Fz* (N)						
1	360	0.14	1	26.30	27.019	2.73
2	534	0.08	2	20.98	21.906	4.41
3	534	0.14	2	32.53	33.476	2.91

$$Fz = 11.699 - 0.049 \times Vc + 235.130 \times f + 5.713 \times ap - 0.133 \times Vc \times f - 2.364 \times Vc \times ap + 50.604 \times f \times ap + 3.955E{-}5 \times Vc^2 - 507.118 \times f^2 - 0.482 \times ap^2 \quad (6)$$

$$Pc = -13.467 + 0.123 \times Vc - 1178.538 \times f - 44.084 \times ap + 0.864 \times Vc \times f + 0.164 \times Vc \times ap + 357.261 \times f \times ap - 3.349E{-}4 \times Vc^2 - 4569.823 \times f^2 - 1.625 \times ap^2 \quad (7)$$

$$MRR = 147.431 - 0.320 \times Vc - 921.333 \times f - 73.707 \times ap + 2 \times Vc \times f + 0.160 \times Vc \times ap + 460.667 \times f \times ap \quad (8)$$

The previous models can be used to predict surface roughness (*Ra*), cutting force (*Fz*), cutting power (*Pc*), and material removal rate (MRR) in the range of selected cutting conditions. Figure 10a–d illustrates the differences between the measured and predicted responses of *Ra*, *Fz*, *Pc*, and MRR, respectively. These figures indicate that the quadratic models are capable for representing the system under the given experimental domain. The comparison results prove that the predicted values of different technological studied parameters are closer to those readings recorded experimentally.

In order to better understand the interaction effect of variables on response factors, 3D plots for the measured responses and contour graphs were plotted based on the model equations (Eqs. (5) to (8)). Since each model had three variables, one variable was held constant at the center level for each plot; therefore, a total of four response surface plots were produced for the responses (Figs. 11, 12, 13, and 14).

Figure 11a, b shows that the effect of *Vc* on *Ra* is negligible compared to the effects of *f* and *ap*. Figure 11c shows that the increase of both *f* and *ap* lead to the increase of *Ra*. However, it is noted that the effect of feed rate is more important as it was demonstrated by V.N. Gaitonde et al. [17].

Figure 12a, b reveals that the effect of the *Vc* on *Fz* is not significant. Figure 12c illustrates the interaction effect between *f* and *ap*. In fact, at low value of *ap*, the

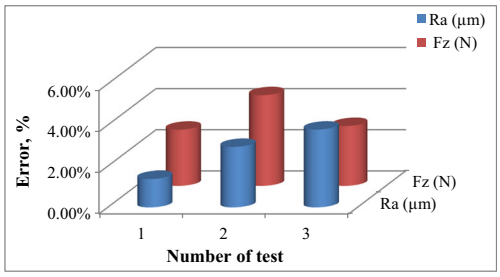

Fig. 15 Verification results for the responses machining on *Ra* and *Fz*

Table 8 Performance of ANN structures of *Ra* model

	Learning		Validation	
Nodes number Input-hidden-output	R^2	RMSE	R^2	RMSE
3-5-1	*0.9891*	*0.0741*	*0.9948*	*0.053*
3-4-1	0.989	0.992	0.994	0.042
3-4-1	0.982	0.099	0.994	0.042
3-3-1	0.995	0.048	0.920	0.214
3-7-1	0.946	0.240	0.999	0.021
3-8-1	0.964	0.196	0.905	0.254
3-9-1	0.999	0.005	0.926	0.321
3-12-1	0.999	0.001	0.919	0.334
3-13–1	0.981	0.129	0.581	0.764

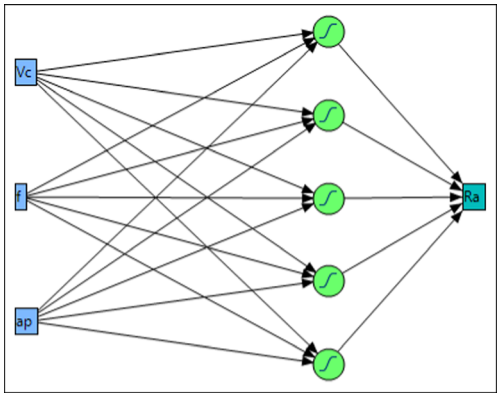

Fig. 16 Neural architecture chosen for *Ra*

influence of *f* is not significant. Conversely, when large values of *ap* are used, the effect of *f* becomes important. It can be concluded that *f* exhibits the maximum influence on cutting force (Table 4).

Figure 13 shows the estimated response surface for power (*Pc*) in relationship with the cutting parameters *ap* and *f*, while *Vc* was kept at the middle level. According to the figures, it can be observed that the cutting power increases with the increase of the three input parameters (*Vc*, *f*, and *ap*), according to Fig. 13b, c, it can be seen that *ap* has more influence on the *Pc*, which confirms the results obtained in Table 5.

From the interaction plot of Fig. 14, it can be observed, on one hand, that the MRR increases with *Vc*, *f*, and *ap*. It should be noted that the maximal material removal rate occurred for the combination of the three highest values of the parameters (*Vc*, *f*, and *ap*).

In order to verify the validation of the quadratic models obtained for *Ra* and *Fz*, confirmation tests were carried out. The results obtained are shown in Table 7 and Fig. 15. It can be clearly seen that the calculated error is very small. The errors between experimental and predicted values for *Ra* and *Fz* are laying 1.38 to 3.78% and 2.73 to 4.41%, respectively.

3.4 Modeling by artificial neural network

The artificial intelligent (AI)-based models, as the artificial neuron network models, are the subject of recent works because of their capability to model the highly nonlinear processes. A neural network consists of a directed weighted graph whose nodes symbolize neurons; these neurons have an activation function to influence other network neurons.

The ANN was initially tested with 03 input training patterns. For each input pattern, the experimental values of surface roughness and tangential cutting force were compared with the respective predicted values. The percentage prediction accuracy of the developed model is given by the following:

$$\delta = \frac{100}{n} \sum_{i=1}^{n} \left| \frac{\left(y_{i,\mathrm{exp}} - y_{i,\mathrm{pred}}\right)}{y_{i,\mathrm{pred}}} \right| \tag{9}$$

where $y_{i,\mathrm{exp}}$ is the experimental value of desired machinability for i^{th} trial, $y_{i,\mathrm{pred}}$ is the predicted value of desired machinability for i^{th} trial, and n is the number of trials.

3.4.1 Modeling of the surface roughness Ra by artificial neural network

The experimental design consists of 27 tests; among them, 23 tests are used for learning the network and 4 are arbitrarily chosen for validating the network. The neural network learning is made by backpropagation algorithm, which is based on the gradient-descent method.

Several network structures were tested as shown in Table 8. According to the correlation coefficient R^2 and the root-mean-square error (RMSE) for both learning and validation sets, the adopted is 3-5-1 (Fig. 16). It is composed of three nodes in the input layer, which corresponds to the number of cutting parameters, five nodes in the hidden layer having a hyperbolic

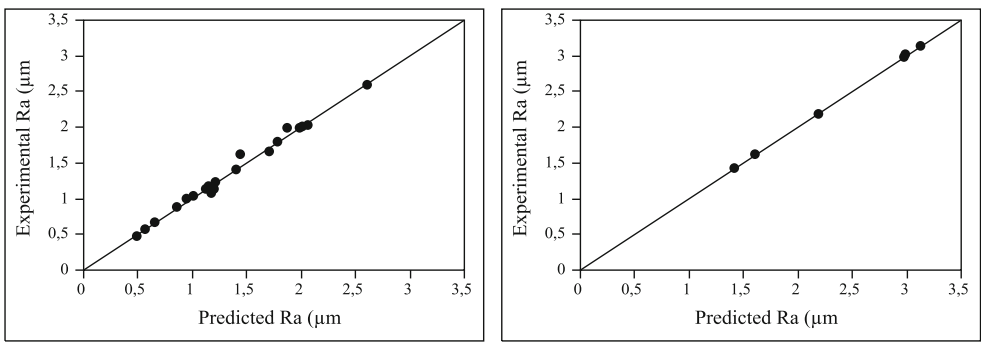

Fig. 17 Comparison of experimental and predicted values for *Ra*

Table 9 Performance of ANN structures of the tangential force (Fz)

Nodes number Input-hidden-output	Learning		Validation	
	R^2	RMSE	R^2	RMSE
3–5-1	*0.9898*	*1.8856*	*0.9998*	*0.2477*
3–4-1	0.997	0.674	0.904	4.367
3–3-1	0.992	1.096	0.861	5.250
3–10-1	0.996	0.761	0.967	2.557
3–9-1	0.853	4.946	0.997	0.717
3–8-1	0.999	0.333	0.962	2.729
3–7-1	0.997	0.636	0.972	2.338
3–6-1	0.999	0.318	0.957	2.909

tangent transfer function, and one node in the output layer having a linear transfer function.

The surface roughness (Ra) ANN model is expressed as follows:

$$Ra = -1.6384 \times H1 + 1.5791 \times H2 + 0.1739 \times H3 - 2.3481 \times H4 - 2.2761 \times H5 + 2.7517 \quad (10)$$

where

$$\left.\begin{aligned} H1 &= \tanh\ (0.5 \times (0.00102 \times Vc - 2.0243 \times f - 1.3173 \times ap + 2.4759));\\ H2 &= \tanh\ (0.5 \times (0.0019 \times Vc + 14.1623 \times f - 0.1530 \times ap - 4.0373));\\ H3 &= \tanh\ (0.5 \times (-0.0044 \times Vc - 6.4026 \times f + 0.3529 \times ap - 2.7273));\\ H4 &= \tanh\ (0.5 \times (0.0032 \times Vc - 13.9206 \times f + 0.7324 \times ap + 2.5319));\\ H5 &= \tanh\ (0.5 \times (-0.0011 \times Vc + 17.0501 \times f + 1.3700 \times ap - 4.7352));\end{aligned}\right\} \quad (11)$$

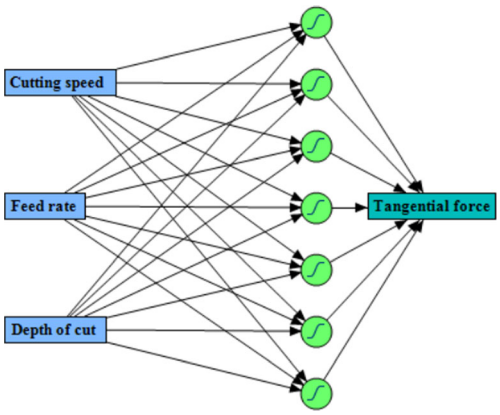

Fig. 18 Neural architecture chosen for Fz

Those terms represent the output of the hidden layer.

Figure 17 presents the plot of the experimental values as a function of their corresponding predicted values. By analyzing this figure, we can notice that the points of intersection between the experimental and the estimated values are very close to the median line for both learning and validation sets (with a slope of 45°), which proves the effectiveness of the ANN model.

3.4.2 Modeling of the tangential force (Fz) by artificial neural network

The same steps are considered to model tangential force (Fz). The statistical results of the tested network structures are presented in Table 9. According to the correlation coefficient R^2 and the root-mean-square error (RMSE) for both learning and validation sets, the adopted architecture is 3-7-1.

The chosen architecture for the ANN model is illustrated in Fig. 18.

The tangential force (Fz) ANN model is expressed as follows:

$$Fz = 126.5419 \times H1 + 16.5034 \times H2 - 6.4844 \times H4 - 100.8435 \times H5 + 59.9123 \times H6 + 41.5666 \times H7 + 44.7858 \quad (12)$$

where

$$\left.\begin{aligned} H1 &= \tanh\ (0.5 \times (0.0006 \times Vc - 11.7481 \times f + 1.4929 \times ap + 1.1212));\\ H2 &= \tanh\ (0.5 \times (-0.0147 \times Vc + 8.4132 \times f - 0.3640 \times ap + 6.5017));\\ H3 &= \tanh\ (0.5 \times (-0.0279 \times Vc + 42.3032 \times f + 2.4317 \times ap - 0.4152));\\ H4 &= \tanh\ (0.5 \times (0.0086 \times Vc + 28.9844 \times f - 2.5376 \times ap - 0.0306));\\ H5 &= \tanh\ (0.5 \times (0.0017 \times Vc - 15.0143 \times f + 0.0078 \times ap + 5.1553));\\ H6 &= \tanh\ (0.5 \times (0.0005 \times Vc + 18.5188 \times f - 0.4125 \times ap - 2.9456));\\ H7 &= \tanh\ (0.5 \times (0.0004 \times Vc + 1.1126 \times f + 1.1126 \times ap + 0.2648));\end{aligned}\right\} \quad (13)$$

Figure 19 illustrates the plot of the experimental values as a function of their corresponding predicted values. It is well seen that the majority of the intersection points are close to the median line, which confirm the robustness of the ANN modeling technique.

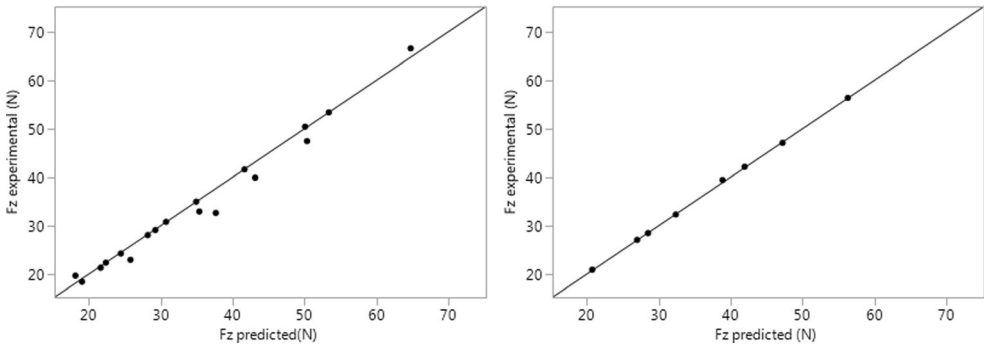

Fig. 19 Comparison between experimental and predicted values for *Fz*

3.5 Comparison between artificial neural network and root-mean-square models

Table 10 presents the coefficients of determination (R^2) of both *Ra* and *Fz* models developed by using response surface methodology (RSM) and artificial neural networks (ANNs).

It is found that the values of R^2 of the ANN models are larger than those of the RSM models, which proves the robustness and the reliability of the ANN method.

To illustrate the comparison between RSM and ANN models, the experimental and the predicted values of surface roughness and tangential force are drawn in Figs. 20 and 21, respectively. It is well observed that the predicted values of the ANN models are more close to the experimental values than those of the RSM models.

3.6 3D surface topography

Analysis of the 3D shows that the increase of *f* causes an increase in the surface roughness (Fig. 22). Indeed, it can be shown that the higher is the value of *f*, the higher is the distance between the peaks and the valleys. This can be explained by the fact that the generated surface comprises helicoid furrows resulting from the tool shape and the form of tool part movements. Obviously, the cut grooves in the hardened material are deeper and broader as *f* is higher, implying to cut at the lower values of *f* for surface finishing [27].

Table 10 Correlation coefficients for RSM and ANN

	Correlation coefficients R^2	
	RSM	ANN
Ra (μm)	96.59	99.19
Fz (N)	98.15	99.48

4 Optimization of responses using desirability function approach

The objective of multiresponse optimization is to determine the conditions on the independent variables that lead to optimal or nearly optimal values of the response variables. Desirability appears to have been first proposed as a criterion for response optimization by Harrington et al. [28] and popularized by Derringer and Suich [29].

Desirable ranges between 0 and 1 and desirability of 0, that is to say an elementary desirability taking the value zero, represent an unacceptable configuration for the selected response, while a desirability taking the value 1 represents the case ideal. The simultaneous objective function is a geometric mean of all transformed responses:

$$D = (d_1 \times d_2 \times \ldots \times d_n)^{1/n} = \left(\prod_{i=1}^{n} d_i\right)^{\frac{1}{n}} \quad (14)$$

$$F(x) = -D \quad (15)$$

where *di* is the desirability defined for the i^{th} targeted output and *wi* is the weighting of *di* and *n* is the number of responses in the measure. For simultaneous optimization, each response must have a low value and a high value assigned to each goal.

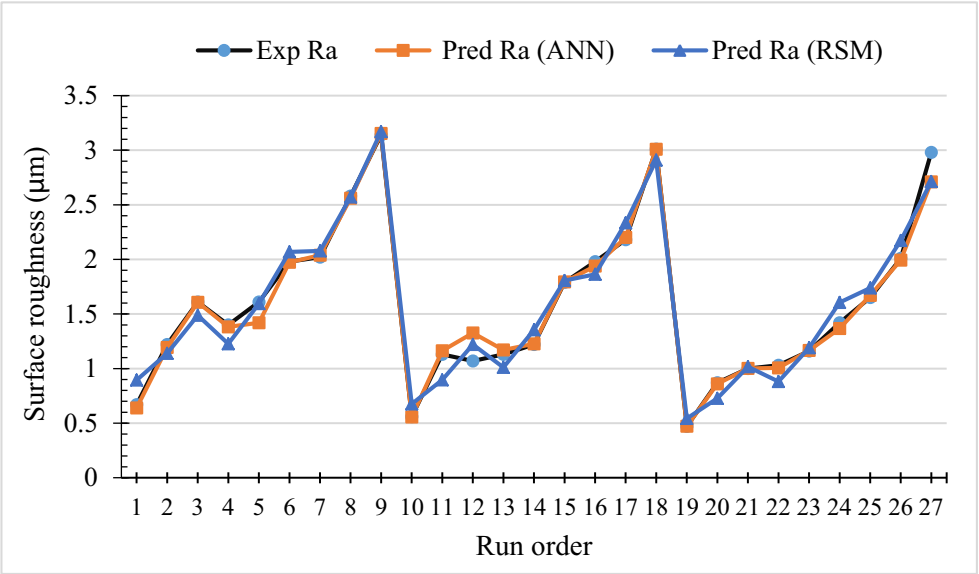

Fig. 20 Comparison between the experimental and predicted results using ANN and RSM for *Ra*

In the case of searching for a *maximum*, the desirability is rewritten as follows:

$$\begin{cases} d_i = 0 \text{ if response} < \text{low value} \\ 0 \le d_i \le 1 \text{ as response varies from low to high} \\ d_i = 1 \text{ if response} > \text{high value} \end{cases} \quad (16)$$

In the case of searching for a *minimum*, the desirability can be defined by the following equations:

$$\begin{cases} d_i = 1 \text{ if response} < \text{low value} \\ 1 \le d_i \le 0 \text{ as response varies from low to high} \\ d_i = 0 \text{ if response} > \text{high value} \end{cases} \quad (17)$$

Here, three optimization approaches are considered. They are called the "quality optimization" and "productivity optimization," and the last one is the combination between the two predicted optimizations. The first

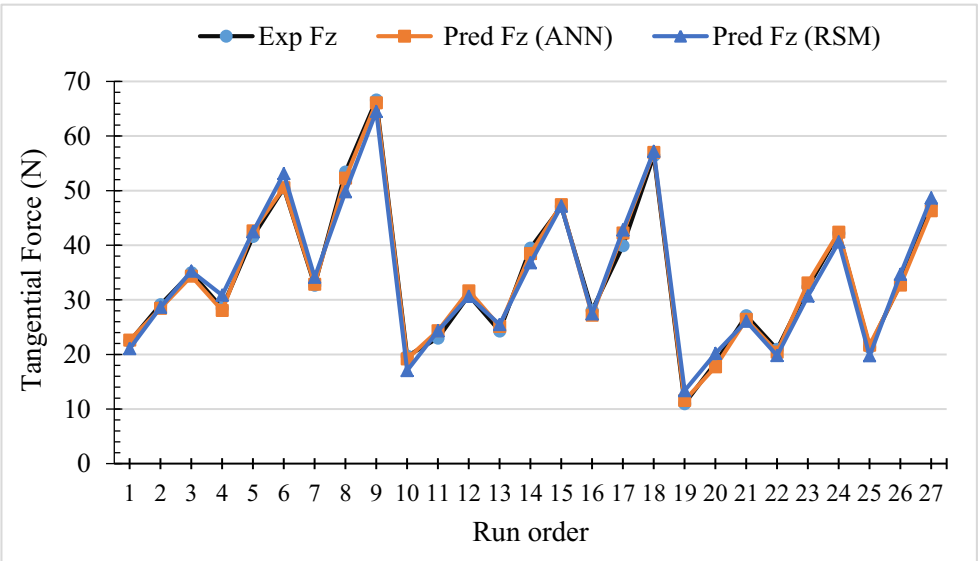

Fig. 21 Comparison between the experimental and predicted results using ANN and RSM for *Fz*

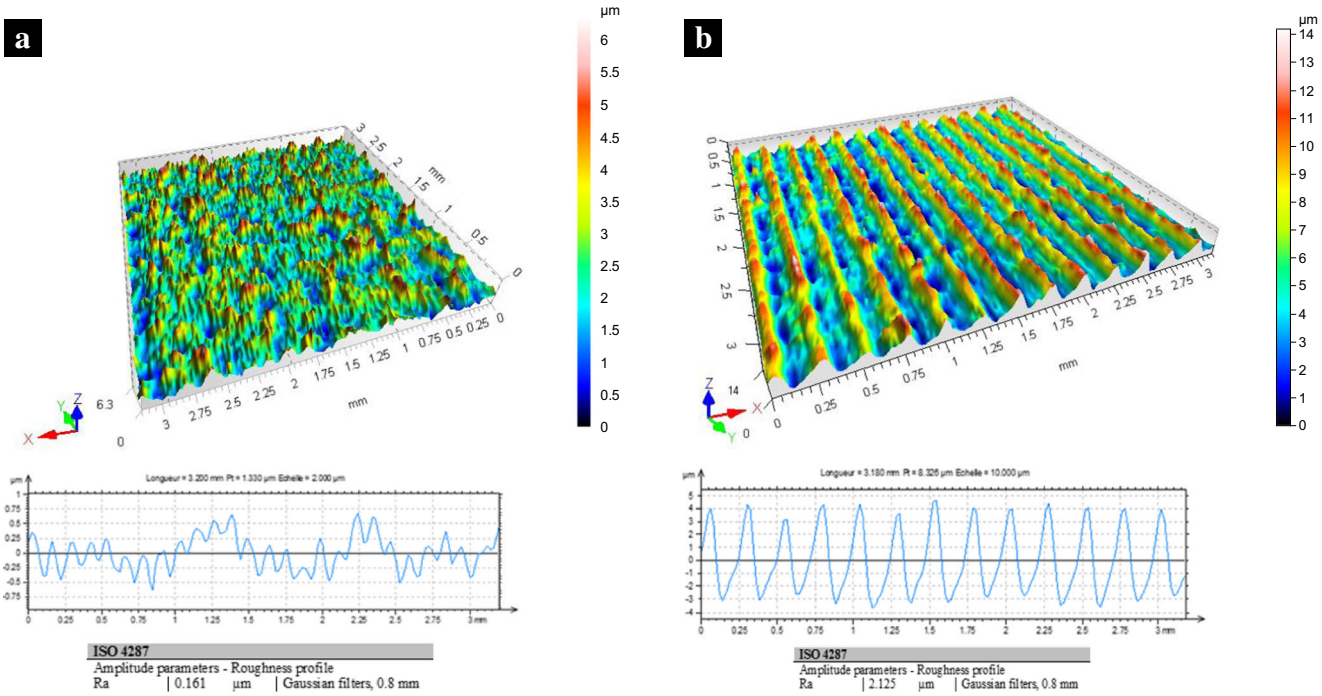

f= 0.08 mm/rev and Vc=440m/min

f= 0.24 mm/rev and Vc=440m/min

Fig. 22 3D topography for surface roughness *Ra*

consists to find the minimum of the surface roughness (*Ra*). In the second, we seek the maximum of MRR. The last is to get the minimum of surface roughness as well as cutting force and cutting power and the maximum of the MRR at the same time. The factor ranges defined for each optimization are summarized in Table 11.

In the case of the third optimization, an interesting advantage consists to have a high productivity and a good surface quality at the same time, and this is what it is aimed in the industry. The contour graph is presented in the Fig. 23; it presents the optimal values of *Vc*, *f*, and *ap* whether that plot shows the increase after the number of revolutions and feed spindle in increasing the opportunity value of MRR and *Ra*.

Figure 24 and Table 12 show the results for the three optimization approaches. The values of the optimal cutting parameters for the combined optimization are as follows: *Vc* = 628 m/min, *f* = 0.097 mm/rev, and *ap* = 1.80 mm. The optimized surface roughness and

Table 11 Goals and factor ranges for optimization of quality, productivity, and combined

Constraints								
Name	Goal	Lower limit	Upper limit	Lower weight	Upper weight	Importance		
						Quality	Productivity	Combined
Vc (m/min)	In range	314	628	1	1	3	3	3
f (mm/rev)	In range	0.08	0.24	1	1	3	3	3
ap (mm)	In range	1	3	1	1	3	3	3
Ra (µm)	Minimize	0.47	3.14	1	1	*5*	None	*5*
Fz (N)	Minimize	10.99	66.6	1	1	None	None	*1*
Pc (W)	Minimize	115.03	496.96	1	1	None	None	*1*
MRR (cm^3/min)	Maximize	25.12	452.16	1	1	None	*5*	*5*

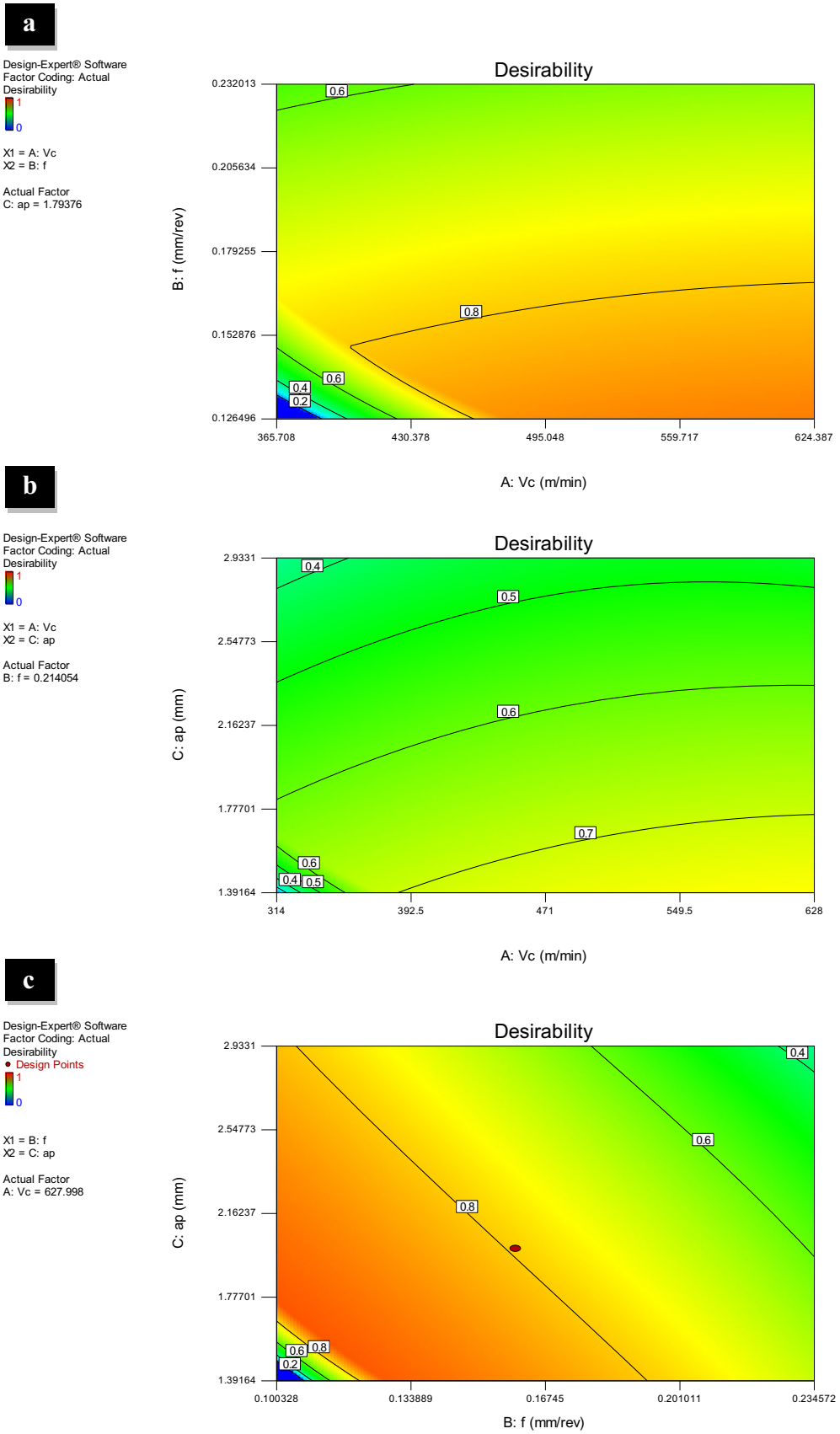

Fig. 23 Contour graphs of desirability: **a** *ap* = 1 mm, **b** *f* = 0.097 mm/rev, and **c** *Vc* = 628 m/min

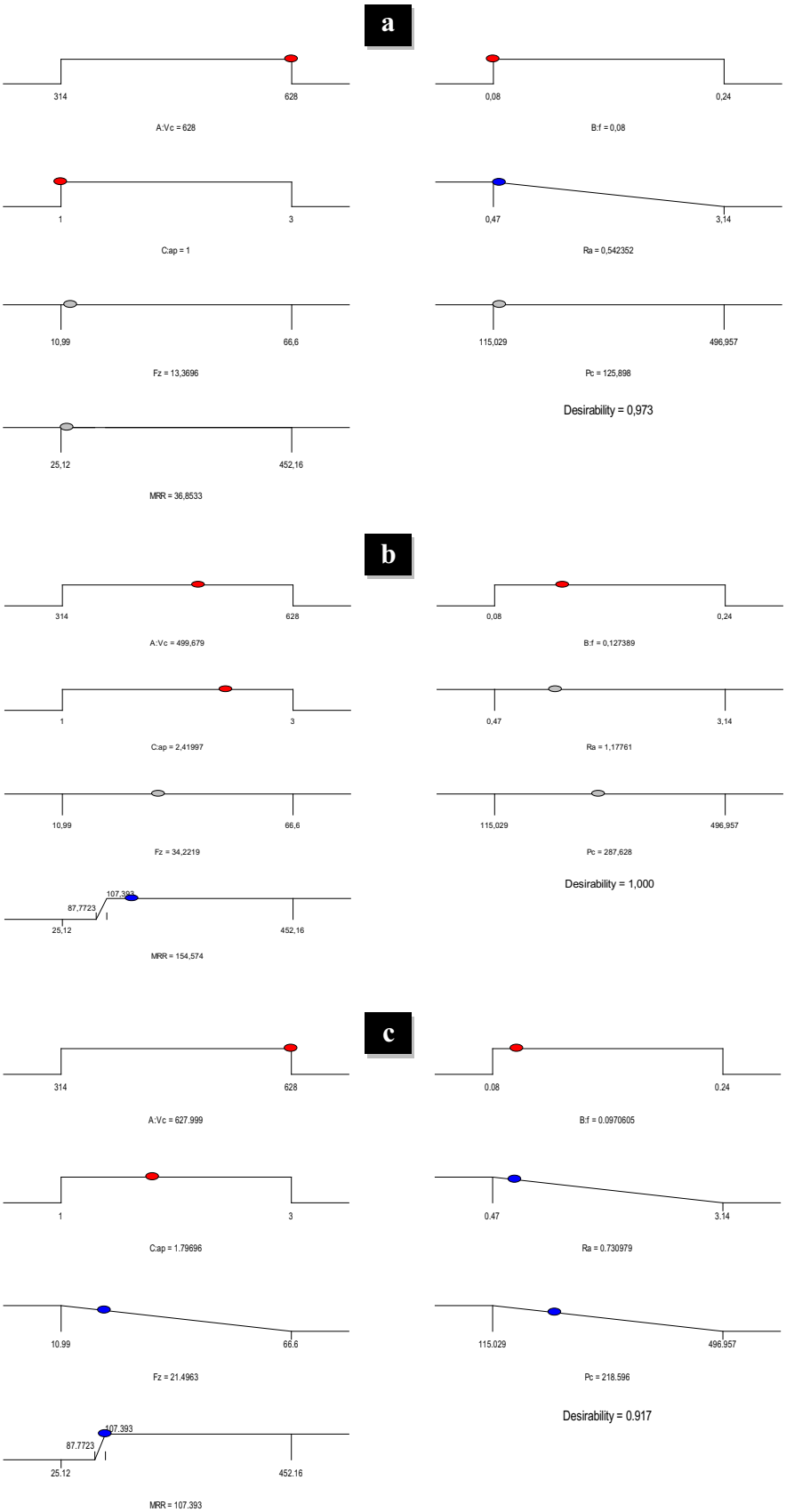

Fig. 24 Ramp function graph for cutting force components and *Ra*, *Fz*, *Pc*, and MRR combined optimization

Table 12 Summary of values obtained for the three case optimizations

Optimization	*Vc* (m/min)	*f* (mm/rev)	*ap* (mm)	*Ra* (μm)	*Fz* (N)	*Pc* (W)	MRR (cm^3/min)	Desirability
Productivity	440	0.24	3	–	–	–	318.453	1.000
Quality	628	0.08	1	0.542	–	–	–	0.973
Combined	628	0.097	1.80	0.731	21.487	218.598	107.393	0.917

the material removal rate are as follows (*Ra* = 0.731 μm and MRR = 107.394 cm^3/min).

5 Conclusion

This study focuses on the modeling and determination of the optimum cutting conditions leading to minimum of surface roughness, cutting force, cutting power, and maximum of productivity. The case of the turning of the POM C was studied. Based on the results discussed previously, the following conclusions could be drawn:

1. The results of the ANOVA analysis for *Ra* proved that the *f* is the most important factor affecting *Ra* followed by *ap* and *Vc*. Their contributions are 66.41, 19.70, and 5.28%, respectively.
2. Tangential cutting force (*Fz)* was highly affected by the *ap* and *f*, and their contributions are 45.41 and 31.09%, respectively. For the cutting power, the three classical input cutting parameters were found significant on *Pc*. Nevertheless, *ap* is the most significant factor with 47.81% of contribution, followed by *f* and *Vc*. Their contributions are of 30.50 and 12.63%, respectively.
3. The material removal rate (MRR) was found affected by *ap* and *f* with same contributions of 37%, followed by *Vc* with contribution of 16.55%. The parameter process interaction contributions were significant.
4. The ANOVA results were confirmed by the Pareto chart and the 3D response surface.
5. The correlation coefficients of the predictive models of *Ra*, *Fz*, *Pc*, and MRR were *found* to be about 96. 59, 98.15, 98.15, and 99.53%, respectively. Therefore, the developed models are reliable and they represent an important industrial interest, since they help to make predictions within the range of the actual experimentation.
6. The results of the confirmation tests show that the developed models are effectively able to predict output responses, with a percentage error value less than 4.41%.
7. The values of R^2 of the ANN models are larger than those of the RSM models, which proves the robustness and the reliability of the ANN method.
8. The optimal cutting parameters, leading to minimal surface roughness in case of finish turning, are as follows: *Vc* = 628 m/min, *f* = 0.08 mm/rev, and *ap* = 1 mm.
9. In case of maximizing the material removal rate, i.e., maximizing the productivity, which is recommended in roughing machining, efficient cutting parameters are *Vc* = 628 m/min, *f* = 0.08 mm/rev, and *ap* = 3 mm.
10. For the combined optimization carried out to compromise simultaneously between the quality and the productivity, optimal conditions are *Vc* = 628 m/min, *f* = 0.097 mm/rev, and *ap* = 1.80 mm.
11. The 3D topographic map of the machined surface is an important investigation tool. It allows the visualization and the confirmation of the feed rate effect on surface roughness.

ANN, artificial neural network; ANOM, analysis of means; ANOVA, analysis of variance; *ap*, depth of cut (mm); cont %, contribution ratio (%); DF, desirability function; DoF, degrees of freedom; *f*, feed rate (mm/rev); *Fa*, axial force (N); *Fz*, tangential force (N); *Fr*, radial force (N); *Fv*, tangential force (N); IHSA, improved harmony search algorithm; MRR, material removal rate (cm^3/min); *Pc*, power (W); *r*, insert nose radius (mm); R^2, determination coefficient; *Ra*, arithmetic mean roughness (μm); RSM, response surface methodology; SS, sequential sum of squares; SC, sum of squares; *Vc*, cutting speed (m/min)

Acknowledgements This work was achieved in the laboratory LMS (Guelma University, Algeria). The authors would like to thank the Algerian Ministry of Higher Education and Scientific Research (MESRS).

References

1. Jiang Q, Zhang LC, Pittolo M (2000) The dependence of surface finish of a spectacle polymer upon machining conditions. Progress of Machining Technology. Aviation Industry Press, Beijing, pp. 7–12
2. Dusunceli N, Colak OU (2008) The effects of manufacturing techniques on visco-elastic and viscoplastic behavior of high density polyethylene (HDPE). Mater Design 29:1117–1124
3. Bestared M (2006) Etude de la durabilité de pièces thermoplastiques. Application au polyoxyméthylène, thèse de doctorat à l'E.N.S.A.M, École Nationale Supérieure d'Arts et Métiers, Centre de Paris
4. Yallese MA, Boulanouar L, Chaoui K (2004) Usinage de l'acier 100Cr6 trempé par un outil en nitrure de bore cubique. Mécanique & Industries 5:355–368

5. Hessainia Z, Yallese MA, Chaoui K, Mabrouki T, Rigal JF (2013) On the prediction of surface roughness in the hard turning based on cutting parameters and tool vibrations. Measurement 46:1671–1681
6. Azizi MW, Belhadi S, Yallese MA (2012) Surface roughness and cutting forces modeling for optimization of machining condition in finish hard turning of AISI 52100 steel. J Mech Sci Technol 26: 4105–4114
7. Bensouilah H, Aouici H, Meddour I, Yallese MA, Mabrouki T, Girardin F (2016) Performance of coated and uncoated mixed ceramic tools in hard turning process. Measurement 82:1–18
8. Aouici H, Yallese MA, Fnides B, Mabrouki T (2010) Machinability investigation in hard turning of AISI H11 hot work steel with CBN tool. MECHANIKA 86:1392–1207
9. Hessainia Z, Yallese MA, Bouzid L, Mabrouki T (2015) On the application of response surface methodology for predicting and optimizing surface roughness and cutting forces in hard turning by PVD coated insert. Int J Ind Eng Comput 6:267–284
10. Xiao KO, Zhang LC (2002) The role of viscous deformation in the machining of polymers. Int J Mech Sci (Pergamon) 44:2317–2336
11. Davim JP, Mata F (2007) A comparative evaluation of the turning of reinforced and unreinforced polyamide. Int J Adv Manuf Technol 33:911–914
12. Keresztes, Kalacska, Zsidai, Dobrocsi (2011) Machinability of engineering polymers‖, Sustainable Construction and Design, pp. 106–114.
13. Kaddeche M, Chaoui K, Yallese MA (2012) Cutting parameters effects on the machining of two high density polyethylene pipes resins. Mechanics & Industry 13:307–316
14. Jagtap TU, Hemant AM (2015) Machining of plastics: a review. International Journal of Engineering and General Science 3:2091–2730
15. Panda MR, Biswal SK, Sharma YK (2016) Experimental analysis on the effect of process parameters during CNC turning on nylon-6/6 using tungsten carbide tool. International Journal of Engineering Sciences & Research Technology 5(4):2277–9655
16. Oktem H, Erzurumlu T, Erzincanli F (2006) Prediction of minimum surface roughness in end milling mold parts using neural network and genetic algorithm. Mater Des 27:735–744
17. Gaitonde VN, Karnik SR, Mata F, Davim JP (2009) Modeling and analysis of machinability characteristics in PA6 and PA66GF30 polyamides through artificial neural network, Journal of Thermoplastic Composite Materials, Vol. 00-2009
18. Lazarevic D, Madic M, Jankovic P, Lazarevic A (2011) Surface roughness minimization of polyamide PA-6 turning by Taguchi method. Journal of Production Engineering 15:1821–4932
19. Madic M, Marinkovic V, Radovanovic M (2012) Mathematical modeling and optimization of surface roughness in turning of polyamide based on artificial neural network. MECHANIKA 18:2029–6983
20. Madic M, Markovic D, Radovanovic M (2012) Optimization of surface roughness when turning polyamide using ANN- IHSA approach. International Journal of Engineering and Technology 4: 432–443
21. Bouzid L, Yallese MA, Chaoui K, Mabrouki T, Boulanouar L (2015) Mathematical modeling for turning on AISI 420 stainless steel using surface response methodology. Proc IMechE Part B: J Engineering Manufacture 229(1):45–61
22. Bouzid L, Boutabba S, Yallese MA, Belhadi S, François G (2014) Simultaneous optimization of surface roughness and material removal rate for turning of X20Cr13 stainless steel. Int J Adv Manuf Technol 74:879–891
23. Meddour I, Yallese MA, Khattabi R, Elbah M, Boulanouar L (2014) Investigation and modeling of cutting forces and surface roughness when hard turning of AISI 52100 steel with mixed ceramic tool: cutting condition optimization. Int J Adv Manuf Technol 77:1387–1399
24. Aouici H, Bouchelaghem H, Yallese MA, Elbah M, Fnides B (2014) Machinability investigation in hard turning of AISI D3 cold work steel with ceramic tool using response methodology. Int J Adv Manuf Technol 73:1775–1788
25. Vijaya MK, Chincholkar AM (2010) Effect of machining parameters on surface roughness and material removal rate in finish turning of ±30 glass fibre reinforced polymer pipes. Mater Des 31:3590–3598
26. Ansari MS, Sharma D, Nikam S (2014) Study of cutting forces and surface roughness in turning of bronze filled polytetrafluoroethylene. International Journal of Advanced Mechanical Engineering 4:2250–3234
27. Yallese MA, Chaoui K, Zeghib N, Boulanouar L (2009) Hard machining of hardened bearing steel using cubic boron nitride tool. J Mater Process Technol 209:1092–1104
28. Harrington EC Jr (1965) the desirability function. Industrial Quality Control 21(10):494–498
29. Derringer G, Suich R (1980) Simultaneous optimization of several response variables. J Qual Technol 12:214–219
30. Aouici H, Yallese MA, Belbah A, Ameur MF, Elbah M (2013) Experimental investigation of cutting parameters influence on surface roughness and cutting forces in hard turning of X38CrMoV5-1 with CBN tool. Sadhana 38:429–445